CYCLONE GLOBAL NAVIGATION SATELLITE SYSTEM (CYGNSS)

Algorithm Theoretical Basis Document **Level 1B DDM Calibration**	**UM Doc. No.**	**148-0137-X1**
	SwRI Doc. No.	**N/A**
	Revision	**1**
	Date	**19 December 2014**
	Contract	**NNL13AQ00C**

Algorithm Theoretical Basis Documents (ATBDs) provide the physical and mathematical descriptions of the algorithms used in the generation of science data products. The ATBDs include a description of variance and uncertainty estimates and considerations of calibration and validation, exception control and diagnostics. Internal and external data flows are also described.

CYCLONE GLOBAL NAVIGATION SATELLITE SYSTEM (CYGNSS)

<table>
<tr><td rowspan="5">Algorithm Theoretical Basis Document
Level 1B DDM Calibration</td><td>UM Doc. No.</td><td>148-0137-X1</td></tr>
<tr><td>SwRI Doc. No.</td><td>N/A</td></tr>
<tr><td>Revision</td><td>1</td></tr>
<tr><td>Date</td><td>19 Dec 2014</td></tr>
<tr><td>Contract</td><td>NNL13AQ00C</td></tr>
</table>

Prepared by:

_______________________________ Date: _______________

Scott Gleason, Southwest Research Institute

Approved by: ________________________________ Date: ____________
Chris Ruf, CYGNSS Principal Investigator

Approved by: ________________________________ Date: ____________
John Scherrer, CYGNSS Project Manager

Approved by: ________________________________ Date: ____________
Randy Rose, CYGNSS Project Systems Engineer

Released by: ________________________________ Date: ____________
Damen Provost, CYGNSS UM Project Manager

REVISION NOTICE

Document Revision History		
Revision	**Date**	**Changes**
PRE-RELEASE DRAFT	17 June 2013	n/a
INITIAL RELEASE	14 January 2014	Add unwrapping of the radar range equation to estimate normalized scattering cross-section from received power. Add detailed error analysis.
Rev 1	19 December 2014	Change L1b DDM units to scattering cross-section in meters^2. Add ancillary data product of scattering area in each DDM bin. Add greater detail about algorithm implementation.

CYGNSS Level 1b DDM Calibration and Error Analysis

This is a portion of the overall Level 1 Calibration Algorithm Theoretical Basis Document (ATBD) describing the Level 1b calibration and error analysis.

I. Level 1b Calibration Approach

The Level 1b calibration is performed after the Level 1a calibration and will use external meta-data to convert the Level 1a mapped power in Watts to a DDM map of BRCS values. This conversion will be done for every DDM and requires the following information at the time every science DDM is collected,

1) The CYGNSS satellite GPS time, position and velocity in the Earth Centered Earth fixed (ECEF) reference frame.
2) The GPS satellite position and velocity in the Earth Centered Earth fixed (ECEF) reference frame.
3) Detailed knowledge of the CYGNSS nadir antenna gain patterns.
4) Attitude information of the CYGNSS spacecraft.
5) The direct signal power levels, as measured from the CYGNSS zenith antenna.

Additional information calculated using the science meta data and used during the Level 1b calibration of each DDM includes,

1) An accurate geolocation of the specular reflection point in the Earth Centered Earth fixed (ECEF) reference frame.
2) Estimate of the GPS satellite transmit power.
3) Estimate of the GPS satellite antenna gain at the surface point observation angle.
4) The path distances between the GPS satellite and surface and between the surface and the CYGNSS receiving spacecraft.
5) The CYGNSS satellite antenna gain projected over the surface glistening zone.
6) The effective scattering area on the surface of each delay/Doppler bin.
7) Atmospheric corrections generated from ground based models.
8) The instrument sampling and processing correction.

The above parameters are then used to estimate values of the bistatic radar cross section using the forward model described below.

II. Forward Model of Scattered Signal Power

A full expression for the GPS scattered signal power has been previously derived and published in 2000 [4], shown in Equation 1. The original representation has been slightly modified in form and variables,

$$P^g_{\hat{\tau},\hat{f}} = \frac{P^T\lambda^2}{(4\pi)^3}\iint\limits_A \frac{G^T_{x,y}\sigma^0_{x,y}G^R_{x,y}}{(R^R_{x,y})^2(R^T_{x,y})^2L_{a1}L_{a2}}\Lambda^2_{\hat{\tau};x,y}S^2_{\hat{f};x,y}dxdy \tag{1}$$

where $P^g_{\hat{\tau},\hat{f}}$ is the coherently processed scattered signal power, in Watts. P^T is the GPS satellite transmit power and $G^T_{x,y}$ is the GPS satellite antenna gain. $G^R_{x,y}$ is the CYGNSS satellite receiver antenna gain. $R^T_{x,y}$ and $R^R_{x,y}$ are the transmitter to surface and surface to receiver ranges, respectfully. L_{a1} and L_{a2} are Atmospheric losses to and from the surface. $\sigma^0_{x,y}$ is the normalized bistatic scattering cross section (BRCS). λ is the GPS signal carrier wavelength (19 cm). $\Lambda_{\hat{\tau};x,y}$ is the GPS signal spreading function in delay and $S_{\hat{f};x,y}$ is the frequency response of the GPS signal. A is the surface integration area. Covering the region of diffuse scattering for each delay Doppler bin. The scattered signal power is processed using a 1ms coherent integration intervals over a range of relative delays $\hat{\tau}$ and Doppler frequencies $\hat{f}$, followed by 1 second of non-coherent averaging.

By performing the surface integration the above expression can be simplified using the effective values of several variables in each bin (other than σ^0) under the integrand of Equation 1, at each delay/Doppler bin,

$$P^g_{\hat{\tau},\hat{f}} = \frac{P^T\lambda^2G^T_{\hat{\tau},\hat{f}} < \sigma^0_{\hat{\tau},\hat{f}} > \bar{G}^R_{\hat{\tau},\hat{f}}\bar{A}_{\hat{\tau},\hat{f}}}{(4\pi)^3(\bar{R}^R_{\hat{\tau},\hat{f}})^2(\bar{R}^T_{\hat{\tau},\hat{f}})^2L_{a1}L_{a2}} \tag{2}$$

where, $\bar{G}^R_{\hat{\tau},\hat{f}}$ = The receiver antenna gain at each delay/Doppler bin. $\bar{R}^T_{\hat{\tau},\hat{f}}$ and $\bar{R}^R_{\hat{\tau},\hat{f}}$ are the range losses at each delay/Doppler bin and $\bar{A}_{\hat{\tau},\hat{f}}$ is the effective surface scattering area at each delay/Doppler bin.

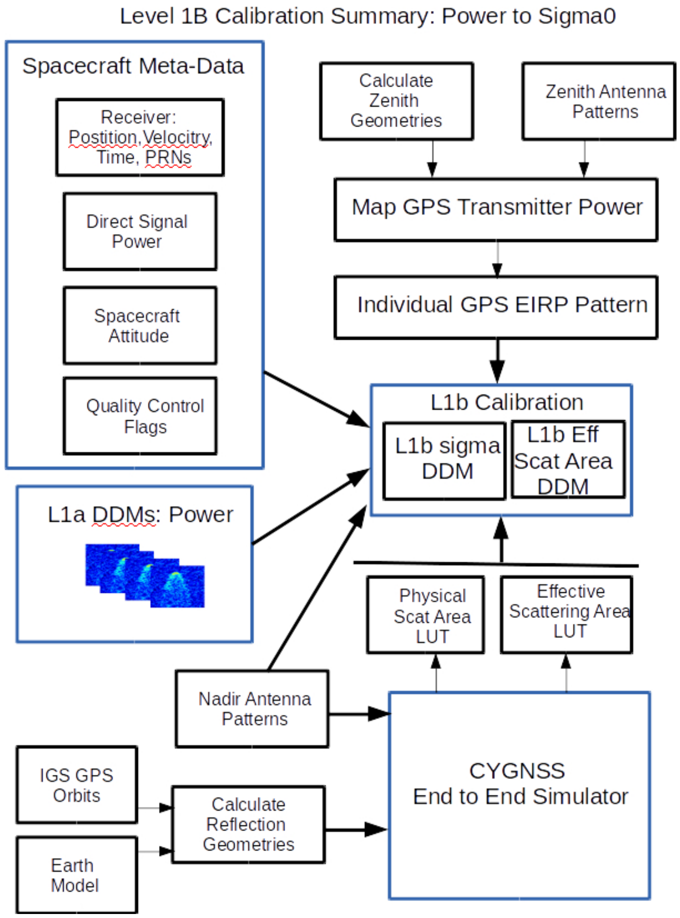

Fig. 1. Overview of CYGNSS Level 1b Calibration.

III. Level 1b Calibration Algorithm: Watts to Sigma0

The Level 1a calibrated DDM represents the received surface signal power in Watts over a range of time delays and Doppler frequencies. Before any geophysical parameters can be estimated these power values must be corrected for non-surface related terms by inverting the forward model shown in Equation 2, based on the familiar radar equation. The CYGNSS Level 1b calibration generates two data products associated with each Level 1a DDM: 1) A bin by bin calculation of the surface bi-static scattering cross section, σ (not normalized by scattering area), and 2) bin by bin values of the effective scattering areas. These two products will allow users to normalize values of σ to values of σ^0 (scattering cross section per meter squared), over configurable surface extents using the effective scattering area of each DDM bin. The values of sigma are corrected for effects of the transmit and receive antennas, range losses and other non-surface related parameters. The effective scattering areas are calculated based on the measurement specific reflection geometry and include the GPS specific delay and Doppler spreading functions. An overview of the CYGNSS Level 1b Calibration is shown in Figure 1

A. *Expression For Bi-static Radar Cross Section*

The final expression for the Level 1b DDM can be derived from the expression of the signal forward model, shown in Equation 2, by solving for the scattering cross section term, $\sigma 0$. As the Level 1b sigma product will not be normalized, we have removed $\bar{A}$ from Equation 2 and replaced the normalized radar cross section σ^0 with a the non normalized, σ. The result expression for σ is,

$$P^{L1b}_{\hat{\tau},\hat{f}} = <\sigma_{\hat{\tau},\hat{f}}> = \frac{P^g_{\hat{\tau},\hat{f}}(4\pi)^3 L_{a1} L_{a2} I_{\hat{\tau},\hat{f}}}{P^T \lambda^2 G^T G^R_{SP} R^{Total}_{SP}} \tag{3}$$

where the individual terms in Equation 3 are as follows,

1) P^g is the Level 1a calibrated signal power at a specific delay ($\hat{\tau}$) and Doppler ($\hat{f}$) bin.
2) R^{Total}_{SP} is the total range loss from the transmitter to the surface and the surface to the receiver at the specular point. When using a relatively small area of of the DDM near the specular reflection point, this value can be approximated as

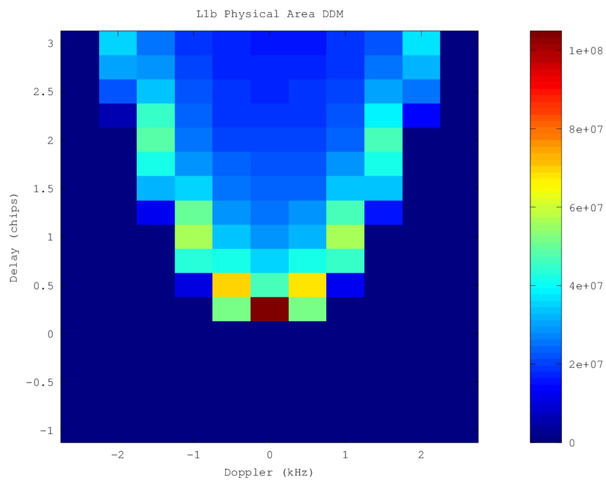

Fig. 2. Physical Scattering Area for a typical DDM reflection geometry. Note that delays before the specular reflection point, and delays at and ahead of specular at increasing Doppler also do not correspond to any physical surface region.

the total range from the transmitter to the specular point to the receiver. This term is included in the denominator as it is calculated as a loss $R^{Total} = \frac{1}{(R^R)^2}\frac{1}{(R^T)^2}$.

3) L_{a1} and L_{a2} are the estimated atmospheric loss corrections from the transmitter to the surface and surface to receiver, respectively.
4) $I_{\hat{\tau},\hat{f}}$ is an additional term used to correct for losses introduced by the DDMI. These include the 2-bit sampling correction and possibly a roll-off correction in the outer Doppler bins due to processing losses inherent in the Zoom Transform Correlator of the instrument [5].
5) P^T and G^T are the GPS satellite transmit power and antenna gain at the specular point. These values are estimated as part of mapping the GPS satellite effective isotropic radiated power (EIRP) pattern of the GPS transmitters.
6) G^R_{SP} is the receiver antenna gain at the specular point. When using a relatively small area of of the DDM near the specular reflection point, this value can be approximated as the receiver antenna gain at the specular point.

B. Calculating Effective and Physical Scattering Areas

A single delay Doppler bin will contain the captured scattered power from a distinct physical region on the ocean surface. For each delay Doppler bin in the DDM this region will vary both in actual physical size (on the ground surface area) and effective area (including GPS spreading functions). The GPS ambiguity functions (in both delay and Doppler) increase the effective area of each delay Doppler bin, causing power to be ”spread” into adjacent delay and Doppler bins from outside the geometry determined physical scattering area. These functions change the overall processed power observed. The physical area of each DDM bin can be calculated as follows,

$$A_{\hat{\tau},\hat{f}} = \iint_A dxdy \tag{4}$$

An example of the physical scattering are for a typical DDM is shown in Figure 2. Note that points up to and before the specular point bin (i.e. at delays shorter than the specular reflection point delay) have no physical surface scattering area. The power received in the bins before the specular point is due to power being spread into these bins by the GPS ambiguity functions from physical areas near the specular point. The effective surface scattering area for each delay/Doppler bin is expressed as the ambiguity function weighted surface integration,

$$\bar{A}_{\hat{\tau},\hat{f}} = \iint_A \Lambda^2_{\hat{\tau};x,y} S^2_{\hat{f};x,y} dxdy \tag{5}$$

where the delay spreading function, $\Lambda_{\hat{\tau};x,y}$ and the Doppler spreading function, $S_{\hat{f};x,y}$, are integrated over the physical surface corresponding to each individual delay/Doppler bin. Figure 3 shows the effective scattering area DDM corresponoding to the physical scattering areas illustrated in Figure 2.

Initial analysis has shown that when only using a relatively small area of the DDM (corresponding to approximately a $25km^2$ area on the surface), it is sufficient to approximate the receive antenna gain, range loss terms and the GPS transmit

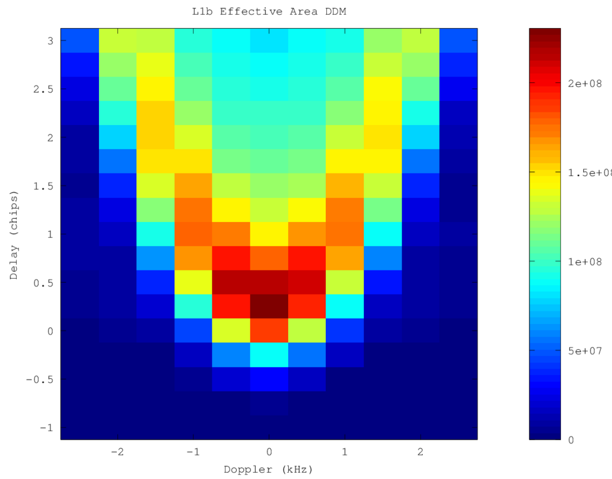

Fig. 3. Effective scattering area corresponding to the physical scattering area shown in Figure 2. This DDM of effective scattering area is a key output product of the Level 1b calibration which allows users to calculate normalized values of σ^0.

antenna power and gain using constant values calculated at the specular reflection point. However, it is recommended that if larger DDMs are used for parameter retrieval at delay and Doppler bins more than 25km distant from the specular point that an improved correction factor for the receiver antenna gain and range loss terms be applied, which account for the surface variations of these parameters over the region of interest.

C. Calculating a Normalized Bi-static Radar Cross Section

The bin by bin DDM of σ and the bin by bin DDM of effective scattering areas can be combined to calculate a normalized radar cross section value, σ^0, over selected regions of the DDM. The resulting expression for σ^0 is,

$$\sigma^0 = \frac{\sigma_{total}}{A_{total}} = \frac{\sum_{i=1}^{N}\sum_{j=1}^{M}\sigma_{\tau_i,f_j}}{\sum_{i=1}^{N}\sum_{j=1}^{M}A_{\tau_i,f_j}} \tag{6}$$

where N and M represent the DDMs bins for delay and Doppler, respectively, used in calculating both the σ and effective scattering area DDMs. During initial testing and validation of the algorithms, including using the E2ES generated 13 day Nature Run DDM sets [2] to test the Level 2 wind retrieval algorithms, a 3x5 area corresponding to $N = 3, M = 5$ centered at the specular point was used to calculate σ^0. This regions corresponds roughly to a $25km^2$ surface resolution, often less, enabling averaging of consecutive DDMs during retrievals [1].

D. Generating GPS Transmit Power and Antenna Gain Look Up Table

The GPS Transmit Power, P_T and transmit antenna gain, G_T, can be estimated using a parametrized model of the GPS antenna pattern and a locus of measurements over the entire bottom sphere of the GPS antenna pattern using direct signal power measurements from the receiver zenith antenna. The baseline GPS antenna patterns will be based on the patterns released in [6]. The theoretical GPS antenna patterns will be generated based on the antenna designs published in [6] and [7].

With the off-boresight angle (θ) and azimuth angles (ϕ) calculated relative to the GPS satellite frame of reference, the GPS transmitter EIRP (including the GPS transmit power P_T and antenna gain G_T) can be estimated using the radar equation and indexed as follows,

$$EIRP^a = (P_T^l G_T^l)(\theta,\phi) = \frac{P_d^l R_D^2 (4\pi)^2}{G_D \lambda^2} \tag{7}$$

where, P_d^l is the received direct signal power from satellite l, R_D is the direct signal range, G_D is the zenith antenna gain and λ is the GPS L1 wavelength.

Flag	Derived From	Threshold	Comment
Reconfiguration during DDM	DDMI flag	on/off	indicates validity of DDM
Calibration/Science DDM	DDMI flag	switch state	indicates type of DDM
Direct signal in DDM	ground based analysis	physical area of DDM	Due to aliasing of the C/A code period
Low range corrected gain	RCG	TBD	Low power signals due to antenna gain and range losses
High incidence angle	θ	60 deg	Region of different scattering model
Large S/C attitude error	S/C roll,pitch,yaw	TBD	Drag or sun pointing manoeuvre
High atmospheric activity	ground based data and models	TBD	Could adversely effect geo-location of SP
GPS antenna gain not confidently estimated	GPS EIRP uncertainty	TBD	Due to gaps or errors in GPS transmiter model
Negative Sigma0 in DDMA	In area near DDM center	Zero	3 delay and 5 Doppler bins

TABLE I
L1B QUALITY CONTROL FLAGS SUMMARY.

E. Quality Control Flags

The Level 1b data product will include a set of quality control flags designed to indicate to users potential problems with the data. These flags, the parameters they are derived from and the default threshold values are listed in Table I.

1) Reconfiguration During DDM. This flag is set by the instrument when a configuration change occurs during the 1 second DDM integration interval. During calibration events, this flag will be set to indicate that the DDM is a mixture of the antenna and black body load inputs and should not be used.
2) Calibration/Science DDM. This flag reflects the state of the black body calibration switch. The switch will indicate either the external antenna (science mode) or the black body load as the current input source.
3) Direct Signal in DDM. This flag will be generated in the SOC by analysing the reflection geometry to determine if the direct signal delay and Doppler fall in the same range as the near specular DDM Area (DDMA) used in Level 2 wind retrievals.
4) Low Range Corrected Gain (RCG). This flag indicates if a DDM was collected with a RCG below the threshold which may not meet the wind speed retrieval requirement. This flag is used to indicate a possible weak signal due to low antenna gain and range losses.
5) High Incidence Angle. Reflection geometries resulting in incidence angles greater than a threshold will be flagged.
6) Large Spacecraft Attitude Error. This flag will be set if the spacecraft attitude determination algorithm indicates that the spacecraft is outside its nominal attitude requirement.
7) High Atmospheric Activity. Used to flag potential adverse atmospheric conditions in the signal path that could degrade the quality of the DDM and/or cause errors in the geo-location.
8) Low Confidence in GPS EIRP. This flag will be set by the SOC if the model of the GPS transmitter at a given geometry is not well determined.
9) Negative Sigma0 in DDMA. Physically it is not possible to have a negative sigma0. When this conditions occurs it will be flagged if it falls near the center of the DDM used for L2 wind retrievals.

IV. ERROR ANALYSIS OF THE LEVEL 1B CALIBRATION ALGORITHM

The Level 1b data product consists of the bistatic radar cross section over a range of delay steps and Doppler frequencies. This error analysis concentrates on the uncertainties present in CYGNSS Level 1b calibration algorithm. Each uncertainty in the Level 1b calibration algorithm will be considered an independent uncorrelated error source. The method for this error analysis is based on that presented in Jansen et. al [3] for a microwave radiometer. The equation for generating the Level 1b data product is expressed in 3. The equation is repeated below, with the two atmospheric terms combined, such that

In order to assess the error in the normalized radar cross section, σ^0, expressed in Equation 6, Equation 3 has been normalized by the effective scattering area and considered for DDM bins in a region (within approximately 25 km) near the specular reflection point such that,

$$P_{25km}^{L1b} = <\sigma_{25km}^0> = \frac{P_{25km}^g (4\pi)^3 L_{a1} L_{a2} I}{P^T \lambda^2 G^T G_{SP}^R R_{SP}^{Total} A_{25km}} \tag{8}$$

The total error in the Level 1b DDM is the root sum square (RSS) of the individual errors contributed by the independent terms of Equation 8. Substituting this equation into Equation **??** results in,

$$E(q_i) = \left| \frac{\partial <\sigma_{25km}^0>}{\partial q_i} \right| \Delta q_i \tag{9}$$

where the errors terms are: $q_1 = P_g$, $q_2 = L_{a12}$, $q_3 = R^R$, $q_4 = R^T$, $q_5 = P_T$, $q_6 = G^T$, $q_7 = G^R$ and $q_8 = A$, respectively. The partial derivatives of the individual errors terms can be expressed as,

$$E(P^g_{\hat{\tau},\hat{f}}) = \frac{(4\pi)^3 \big(\bar{R}^R_{\hat{\tau},\hat{f}}\big)^2 \big(\bar{R}^T_{\hat{\tau},\hat{f}}\big)^2 \bar{L}_{a1}\bar{L}_{a2}}{P^T \lambda^2 \bar{G}^T_{\hat{\tau},\hat{f}} \bar{G}^R_{\hat{\tau},\hat{f}} A_{\hat{\tau},\hat{f}}} \Delta P^g_{\hat{\tau},\hat{f}} \tag{10}$$

$$E(L_{a12}) = \frac{P^g_{\hat{\tau},\hat{f}} (4\pi)^3 \big(\bar{R}^R\big)^2 \big(\bar{R}^T\big)^2}{P^T \lambda^2 \bar{G}^T \bar{G}^R A} \Delta L_{a12} \tag{11}$$

$$E(R^R) = \frac{2P^g_{\hat{\tau},\hat{f}} (4\pi)^3 \big(\bar{R}^R\big) \big(\bar{R}^T\big)^2 L_{a12}}{P^T \lambda^2 \bar{G}^T \bar{G}^R A} \Delta R^R \tag{12}$$

$$E(R^T) = \frac{2P^g_{\hat{\tau},\hat{f}} (4\pi)^3 \big(\bar{R}^R\big)^2 \big(\bar{R}^T\big) L_{a12}}{P^T \lambda^2 \bar{G}^T \bar{G}^R A} \Delta R^T \tag{13}$$

$$E(P_T) = \frac{P^g_{\hat{\tau},\hat{f}} (4\pi)^3 \big(\bar{R}^R\big)^2 \big(\bar{R}^T\big)^2 L_{a12}}{\big(P^T\big)^2 \lambda^2 \bar{G}^T \bar{G}^R A} \Delta P_T \tag{14}$$

$$E(G^T) = \frac{P^g_{\hat{\tau},\hat{f}} (4\pi)^3 \big(\bar{R}^R\big)^2 \big(\bar{R}^T\big)^2 L_{a12}}{P^T \lambda^2 \big(\bar{G}^T\big)^2 \bar{G}^R A} \Delta G^T \tag{15}$$

$$E(G^R) = \frac{P^g_{\hat{\tau},\hat{f}} (4\pi)^3 \big(\bar{R}^R\big)^2 \big(\bar{R}^T\big)^2 L_{a12}}{P^T \lambda^2 \bar{G}^T \big(\bar{G}^R\big)^2 A} \Delta G^R \tag{16}$$

$$E(A) = \frac{P^g_{\hat{\tau},\hat{f}} (4\pi)^3 \big(\bar{R}^R\big)^2 \big(\bar{R}^T\big)^2 L_{a12}}{P^T \lambda^2 \bar{G}^T \bar{G}^R \big(A\big)^2} \Delta A \tag{17}$$

The error analysis was performed for both the below 20 m/s wind case (assuming a $\sigma 0$ of 20 dB) and greater than 20 m/s winds case (assuming a $\sigma 0$ of 12 dB) to fully understand the possible errors in both wind retrieval groups. Initially, the errors due to the receiver antenna gain, G_R, were estimated using a Monte Carlo simulation. The simulation was run using the error estimates listed in Table II as input conditions, and then the 1-σ error statistics of the antenna gain were calculated as a function of antenna gain magnitude.

Error Term	**Error Magnitude**	**Comment**
Space Craft Pointing Knowledge	0.73 deg (1 σ)	From AOCS Analysis (with Star Tracker)
Star Tracker Optical/Mechanical Boresight Misalignment	0.4 deg (1 σ)	Rough Estimate From Mechanical Analysis
Star Tracker to Nadir Antenna Misalignment	0.4 deg (1 σ)	Rough Estimate From Mechanical Analysis
Mechanical-Electrical Nadir Antenna Boresight Misalignment	0.5 deg (1 σ)	Expected Antenna Calibration Accuracy
Repeatability of Antenna Gain	-3.0 dB (1 σ)	Based on 18 FM Antenna Pattern Measurements
Antenna Pattern Uncertainty	0.25 dB (1 σ)	Expected Antenna Calibration Accuracy
Margin	0.2 dB	
RSS (1 σ) Antenna Gain Error + Margin	0.40 dB	From Monte Carlo Simulation

TABLE II
ERROR ALLOCATIONS FOR THE RECEIVER ANTENNA GAIN.

Errors for the remaining terms of the Level 1b calibration were arrived at using best estimates. Table III shows the resulting error values used for the low wind and high wind cases, respectively.

Subsequently, the rolled up Level 1 calibration error can be estimated using the Equations above, which consist of taking the root sum square of all of the individual error terms, including the total error estimate from the Level 1a calibration. Quantitative values for each or the error components listed above and the RSS total for both scenarios are shown in Table IV.

From Table IV the total error in the L1 calibration is estimated to be, 0.69 dB (1-sigma) and 0.51 dB (1-sigma), for the below and above 20 m/s wind speed cases, respectively.

Error Term	Error in dB (error in %)	Comment
ΔP_g	0.49/0.17	From Level 1a Error Analysis
ΔL_{a12}	0.04 dB	Based on Approximate L-Band Attenuations
ΔR^R	˜1000 meters	Determined by Reflection Geometry
ΔR^T	˜1000 meters	Determined by Reflection Geometry
ΔP_T + ΔG^T	0.4 dB	GPS Tx EIRP error
ΔG^R	0.40 dB	From Monte Carlo Simulation, Table II
ΔA	0.2 dB	Determined by Reflection Geometry

TABLE III
LEVEL 1B CALIBRATION ERROR ANALYSIS INPUT PARAMETERS.

Error Term	L1b error, dB	L1b error, dB	Comment
	Low Winds, Less Than 20 m/s	High Winds, Greater Than 20 m/s	
$E(P_g)$	0.49	0.17	L1a calibration error
$E(L_{a12})$	0.04	0.04	Total atmospheric modelling error
$E(R^R)$ + $E(R^T)$	0.004	0.01	Total range error
$E(P_T)$ + $E(G^T)$	0.40	0.40	GPS Transmiter EIRP error
$E(G^R)$	0.25	0.25	Receiver gain error
LNA Gain Error	0.09	0.09	Error in estimated LNA Gain
$E(A)$	0.20	0.20	Effective scattering area error
Margin	0.20	0.20	
Total RSS L1b Error Plus Margin	0.69	0.51	Rolled up L1a and L1b errors

TABLE IV
LEVEL 1B CALIBRATION ALGORITHM ERRORS (DB).

A. *Error Analysis of GPS EIRP Estimation*

Repeating the analysis using partial derivatives of Equation 7, results in the following error terms,

$$E(P_d) = \frac{R_D^2 (4\pi)^2}{G_D \lambda^2} \Delta P_d \tag{18}$$

$$E(R_D) = \frac{2 P_d R_D (4\pi)^2}{G_D \lambda^2} \Delta R_D \tag{19}$$

$$E(G_D) = \frac{P_d R_D^2 (4\pi)^2}{G_D^2 \lambda^2} \Delta G_D \tag{20}$$

Assuming the following 1 σ errors for each term: ΔP_d = 0.10 dB, ΔR_D = 50 meters, ΔG_D = 0.11 dB, respectively. The error in the direct signal power error is assumed to be the RSS of the LNA gain and noise figure errors from the L1a look up tables. The direct signal range error is assumed to be the maximum expected delay error caused by worst condition atmospheric activity. The zenith antenna gain error will be lower than the nadir antenna gain error (due to its lower gain and more uniform distribution). A value of 20% of the error of the nadir antenna gain results in an error if 0.11 dB.

From Table V the expected 1 σ error in the estimated Effective Isotropic Radiated Power (EIRP) of the GPS transmitter is 0.4 dB, including a small margin.

Error Term	Magnitude, dB	Comment
$E(P_d)$	0.10	Direct signal power error
$E(R_D)$	0.00	Direct range loss error
$E(G_D)$	0.11	Direct antenna gain error
GPS Antenna Modelling Error	0.20	Quality of fit of model to data
Margin	0.15	
Total GPS EIRP Error Plus Margin	0.40	Flows into L1b Error Analysis

TABLE V
LEVEL 1B GPS TRANSMITTER EIRP ERROR ESTIMATE (DB).

REFERENCES

[1] Clarizia, M.P. et al., Wind Speed Retrieval Algorithm for the Cyclone Global Navigation Satellite System (CYGNSS) Mission, Submitted to IEEE Transactions on Geoscience and Remote Sensing, Dec 2014.
[2] O'Brien, A., Gleason S., Johnson J., and C. Ruf, The End-to-End Simulator for the Cyclone GNSS (CYGNSS) Mission, Submitted to IEEE Transactions on Geoscience and Remote Sensing, Dec 2014.
[3] Jansen, M.A., Ruf, C.S. and S.J. Keihm (1995), TOPEX/Poseidon Mircorwave Radiometer (TMR): II. Antenna Pattern Correction and Brightness Temperature Algorithm, IEEE Trans. Geosci. Remote Sens., Vol. 33, No. 1, pp. 138-146, January 1995.
[4] Zavorotny V. and A. Voronovich (2000), Scattering of GPS Signals from the Ocean with Wind Remote Sensing Application . IEEE Trans. Geosci. Remote Sens., Vol. 38, pp. 951-964, March 2000. DOI: 10.1109/36.841977
[5] Jales, P., GNSS-R Algorithm Implimentation Technical Note, Surrey Satellite Technology Limited Internal Document, October 2013.
[6] Marquis, W., The GPS Block IIR/IIR-M Antenna Panel Pattern, Lockheed Martin internal document, publically released, September 2013.
[7] Czopek, F. M., Shollenberger, S., Description and Performance of the GPS Block 1 and II L-Band Antenna and Link Budget, Proceedings of the Institute of Navigation, 1993.
[8] Bar-Sever, Y., A new model for GPS yaw attitude, Journal of Geodesy 70:714-723, 1996.

APPENDIX

A. Transforming Rx to Specular Point Vector to Antenna Frames

In order to calculate the correct receiver antenna gain at the specular point and around the glistening zone, the vector between the receiving satellite and the specular reflection point needs to undergo several transformations. Initially, the vector from the receiver to the specular point is calculated in the Earth Centered Earth Fixed (ECEF) reference frame. Subsequently it is transformed as follows,

1) Transformation from the ECEF frame to the Specular Point Centered frame.
2) Transformation from the Specular Point frame to the Spacecraft Orbit frame or Local Vertical Local Horizontal (LVLH) frame.
3) Transformation from the Spacecraft Orbit Frame to the Spacecraft Body frame based on the Spacecraft attitude matrix.
4) Transformation from the Spacecraft Body frame to the two Nadir Antenna frames based on each antenna transformation matrix.

The general expression to transform a vector, r, from frame A to frame B can be expressed as,

$$\vec{r}_B = T_B^A \vec{r}_A \tag{21}$$

Where, T_B^A is a 3x3 transformation matrix and $\vec{r}_A$ is a 3x1 vector. Applying this general formula to the transformations above results in,

$$\vec{r}_{Spec} = T_{Spec}^{ECEF} \vec{r}_{ECEF} \tag{22}$$

$$\vec{r}_{Orbit} = T_{Orbit}^{Spec} \vec{r}_{Spec} \tag{23}$$

$$\vec{r}_{Body} = T_{Body}^{Orbit} \vec{r}_{Orbit} \tag{24}$$

$$\vec{r}_{Ant} = T_{Ant}^{Body} \vec{r}_{Body} \tag{25}$$

Where, T_{Spec}^{ECEF} is calculated from ECEF positions of the receiver, transmitter and specular point. T_{Orbit}^{Spec} is calculated from the Receiver position and velocity in the Specular Point frame, with Z "down" and X in the approximate direction of the spacecraft velocity vector. T_{Body}^{Orbit} is the spacecraft attitude matrix. T_{Ant}^{Body} is the transformation between the nominal body frame reference and the antenna frame reference. This operation is performed for each of the two nadir antennas.